EGU2020-1783

Forearc building and destruction: a critical interplay between fluid flow, megathrust strength and tectonic underplating

… to the surface

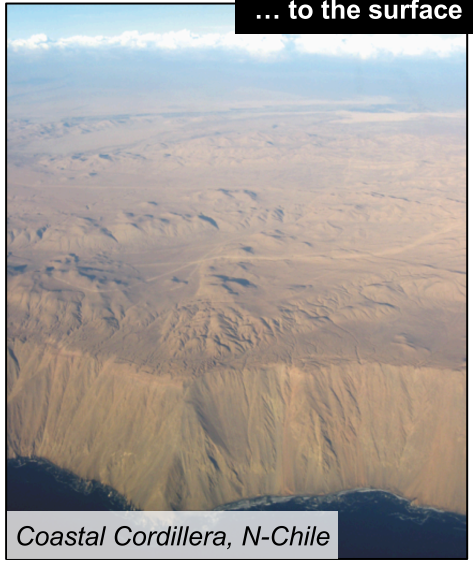

Coastal Cordillera, N-Chile

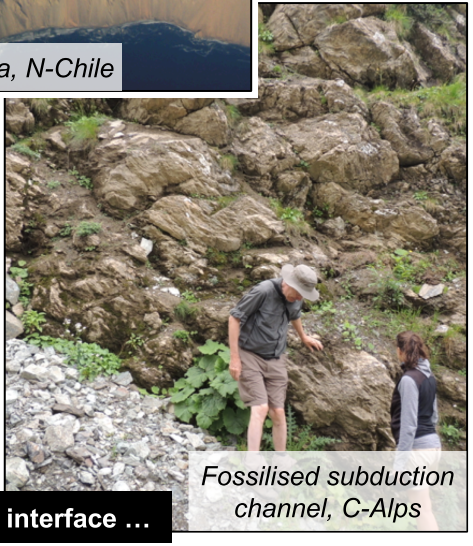

Fossilised subduction channel, C-Alps

From the plate interface …

Armel Menant

GFZ Helmholtz Centre Potsdam, German Research Centre for Geosciences

Samuel Angiboust, Robin Lacassin, Martine Simoes, Raphael Grandin

Institut de Physique du Globe de Paris

Taras Gerya

ETH Zürich

For further information, work also presented at ***DeTect Talk Series*** on Friday 08th May

(http://www.ipgp.jussieu.fr/~klinger/web_Yann/Detect_page/detect.html)

Tectonic underplating: deep accretion at the base of the forearc crust of material dragged down the subduction zone [e.g., *Platt*, 1986]

- Huge mass transfers **suspected along many active margins**

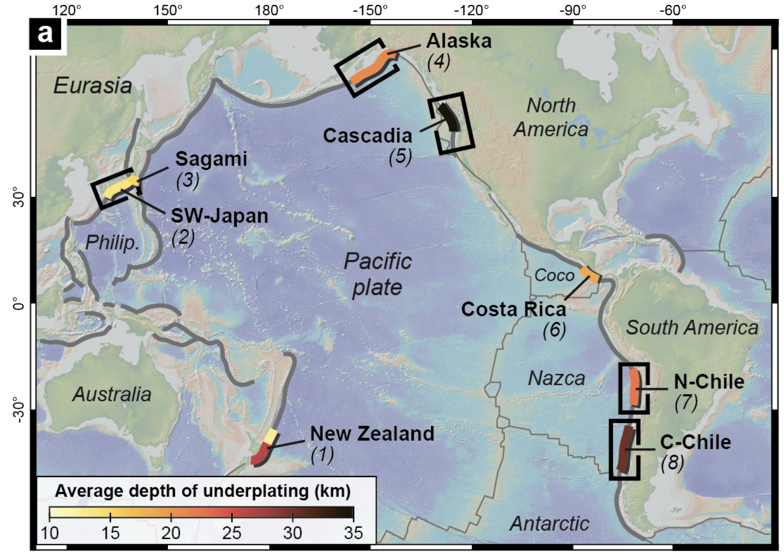

[*Menant et al.*, 2020]

- **Spatial correlation with seismicity** (notably with the downdip end of the seismogenic zone)

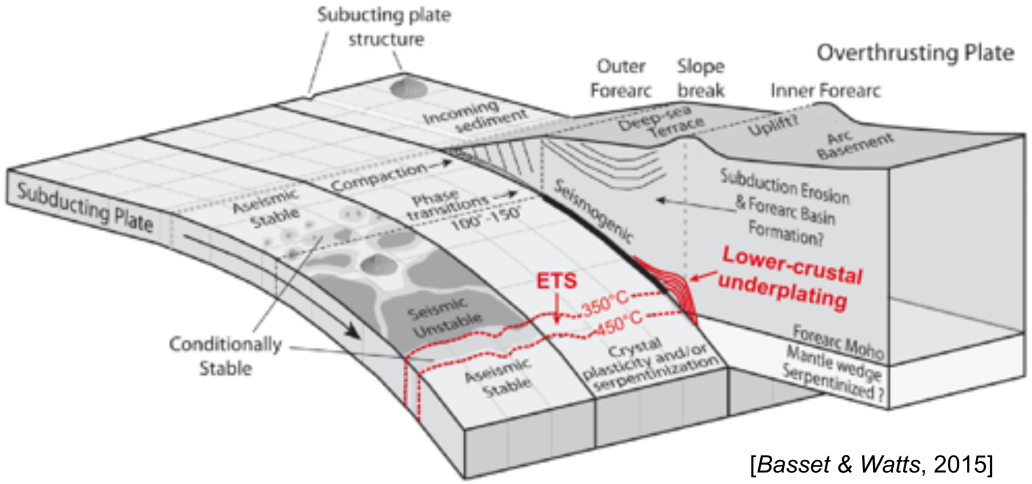

[*Basset & Watts*, 2015]

Characterizing tectonic underplating and associated crustal response from the subduction interface to the surface along active margins

✓ Performing a series of **high-resolution thermo-mechanical models** of ocean-continent subduction zone including **fluid (de)hydration and transport processes**, as well as **fluid-related rheological weakening**

- Field and geophysical evidences of underplating
- Modelling strategy
- Implementation of fluid processes

Supplementary Material

Long-term accretive dynamics along ocean-continent subduction zone

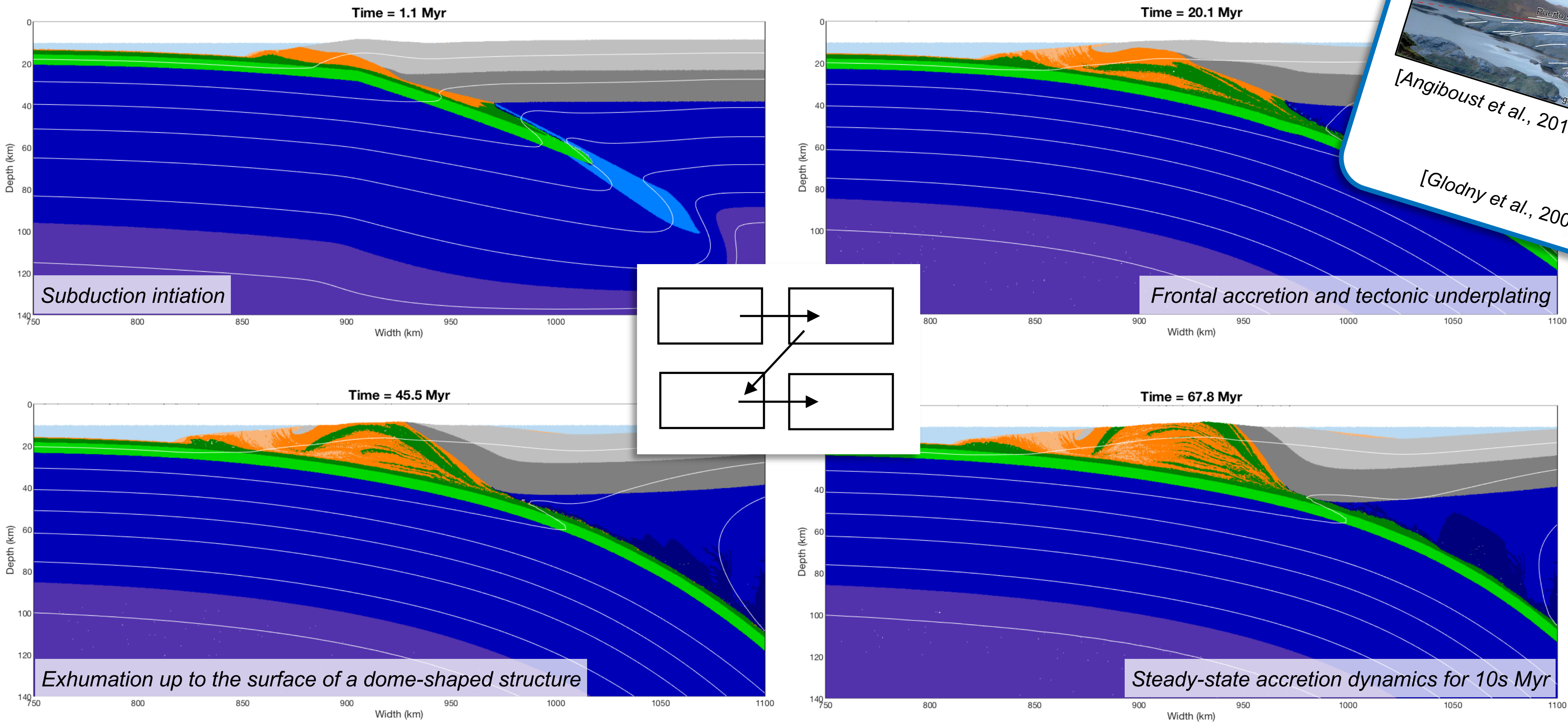

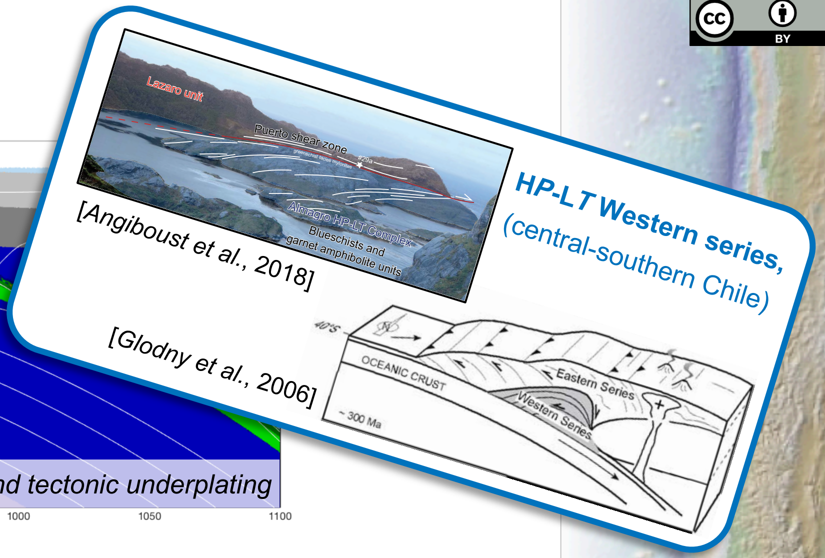

[*Menant et al.*, 2019]

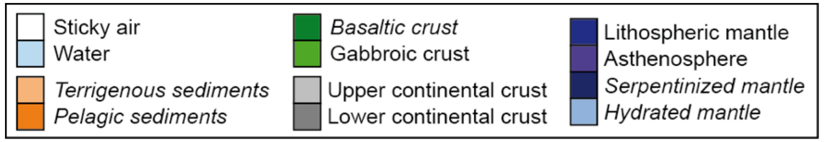

Forearc margin in alternative models

Details on the central-south-Chilean margin

Relation between underplating events and plate interface hydromechanics

➢ **Preferential location of underplating events** (U_{Z1} and U_{Z2}) and **fluid distribution** in the forearc domain

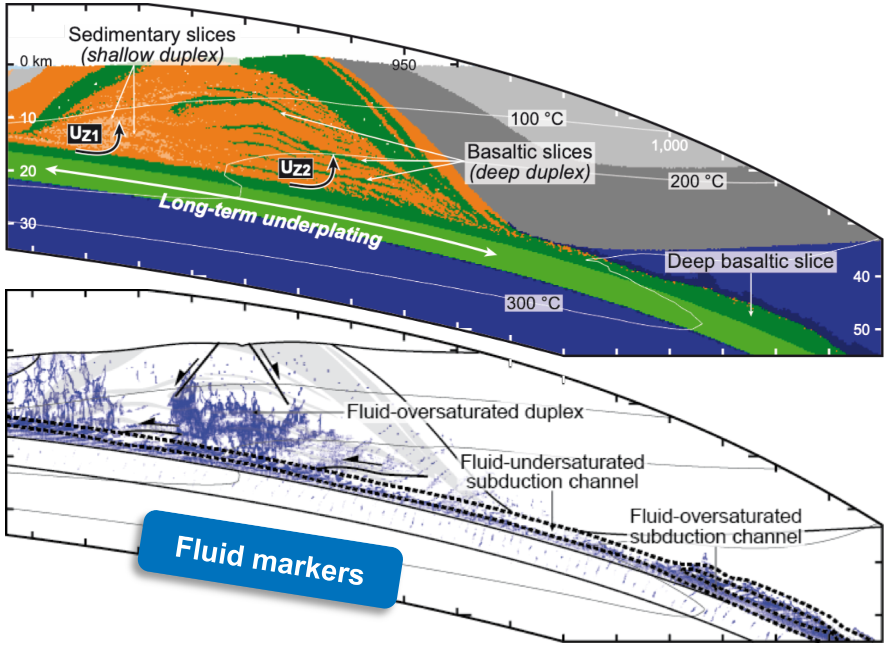

➢ **Shear stress variations along the plate interface**

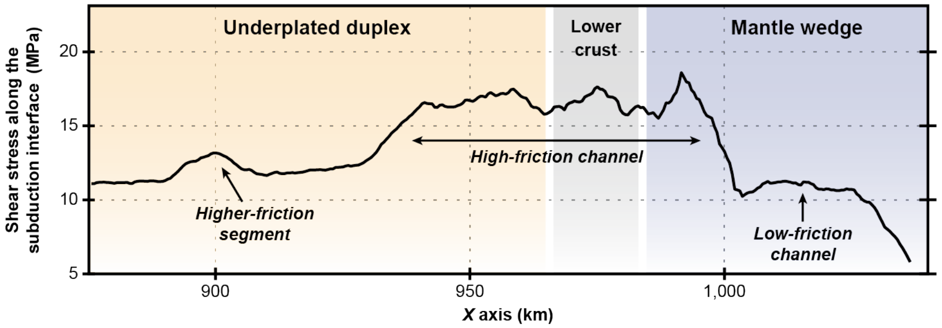

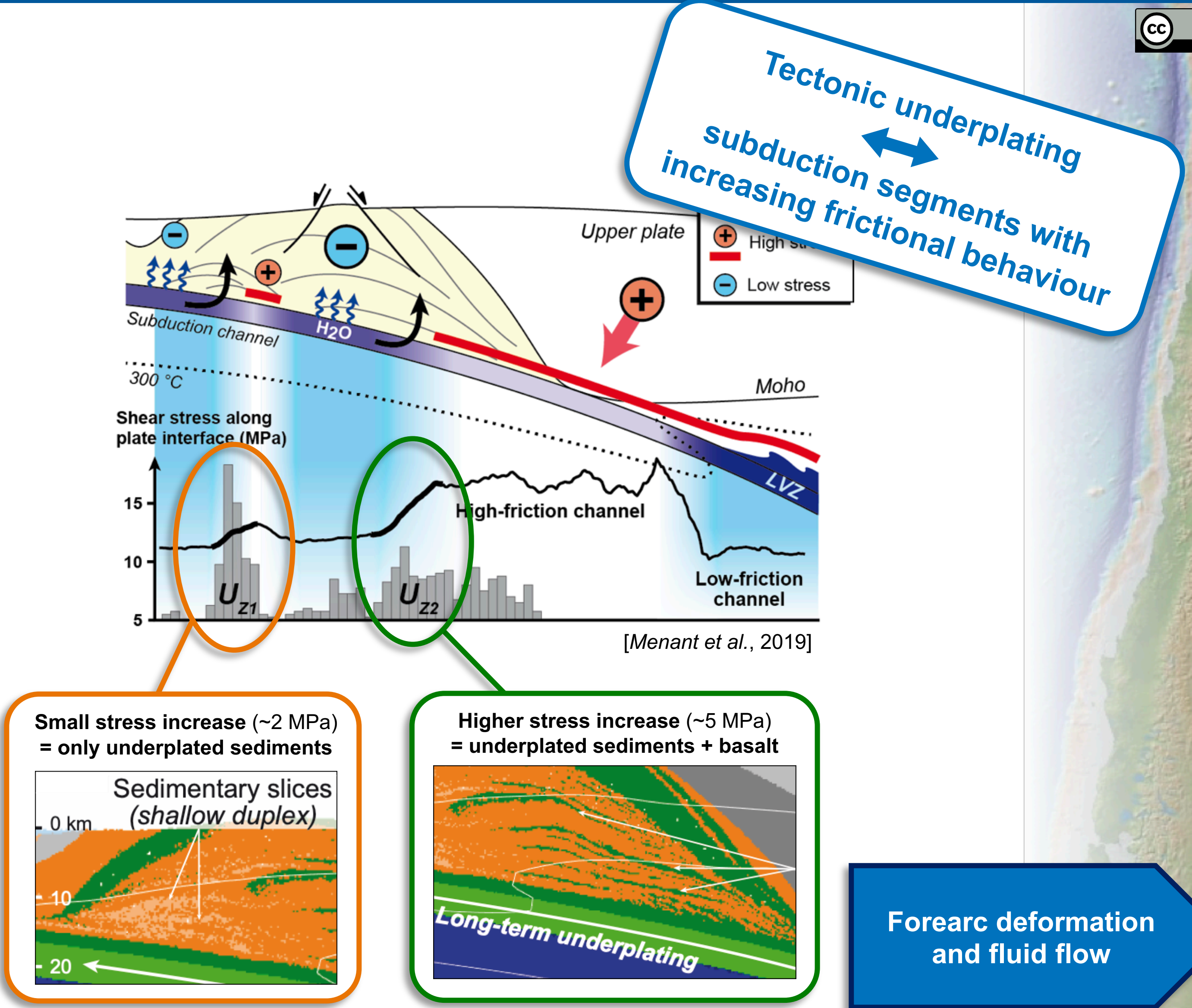

Forearc deformation and fluid flow

The « topographic signature » of tectonic underplating

- Tectonic underplating and long-term forearc topography: **>1,000 m coastal high** and **inner forearc depression**

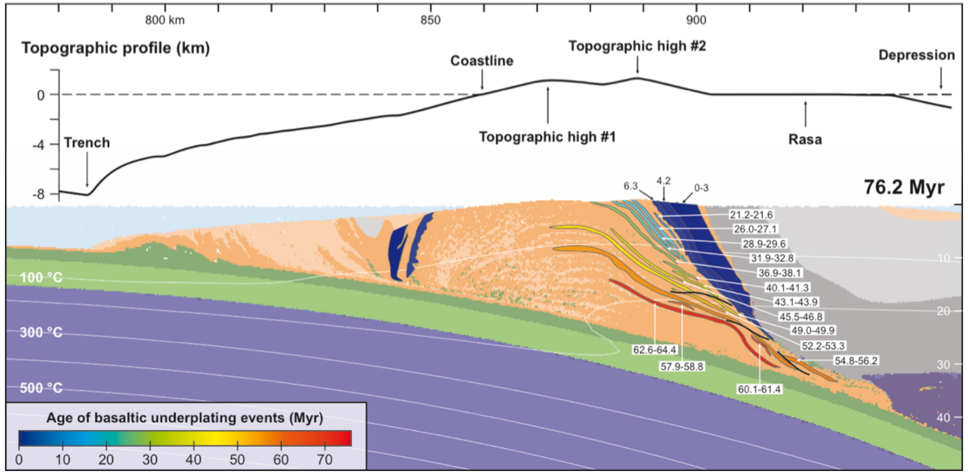

- **Myr-scale vertical oscillations** of the high coastal topography **correlated with underplating events**

~2.8 Myr periodicity

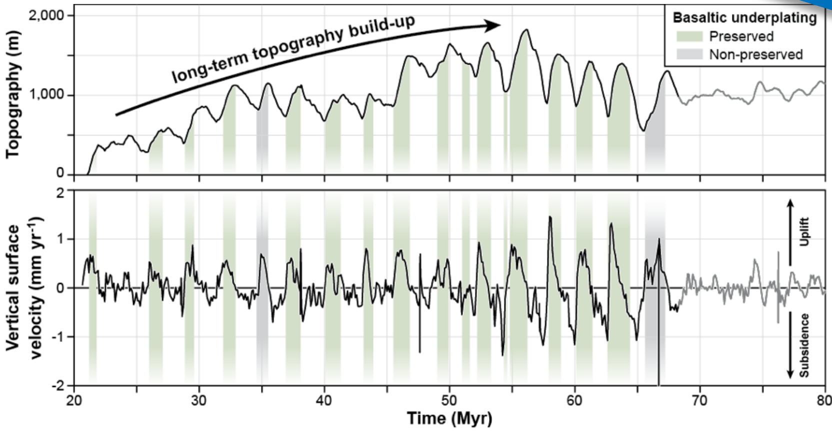

- **Consistent topographic pattern** along accretive margins

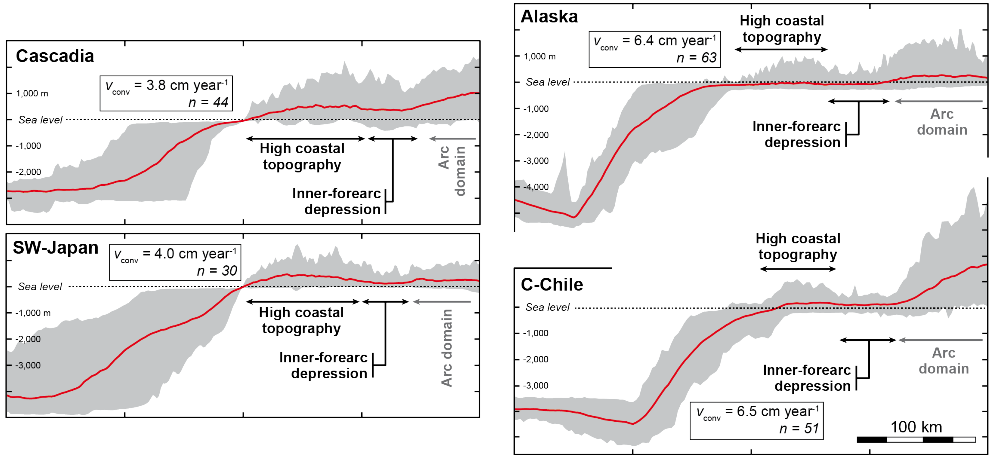

- **Trench-parallel topographic variations as a proxy for temporal variations?**

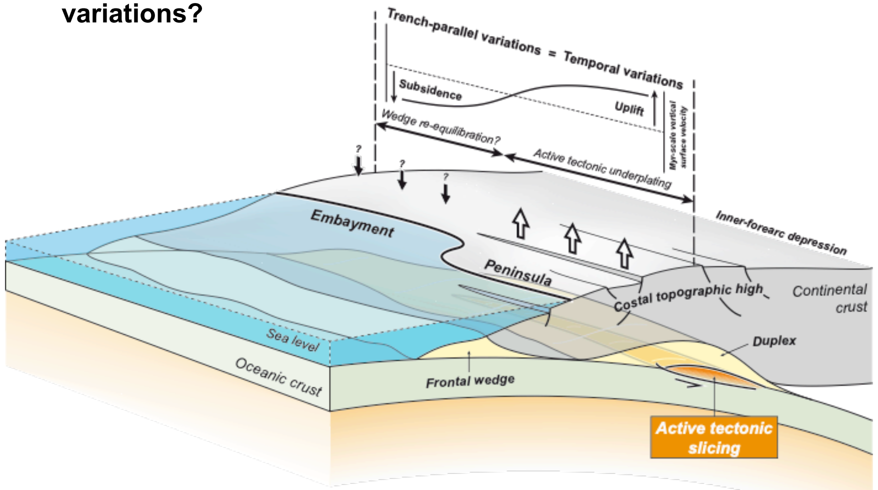

[*Menant et al.*, 2020]

Forearc topography in alternative models

Topographic signal in alternative models

Details on 3D shape of topography

Take-home message(s)

1. **Fluid distribution** plays a critical role on the **mechanical properties of the subduction channel**

2. **The hydromechanical properties** of the interface control the **location, amount and nature of accreted material** at the base of the forearc crust

3. **Tectonic underplating** is responsible for a **Myr-scale topographic signal** leading to the growth of a high forearc topography and **transient emergence of coastal promontories**

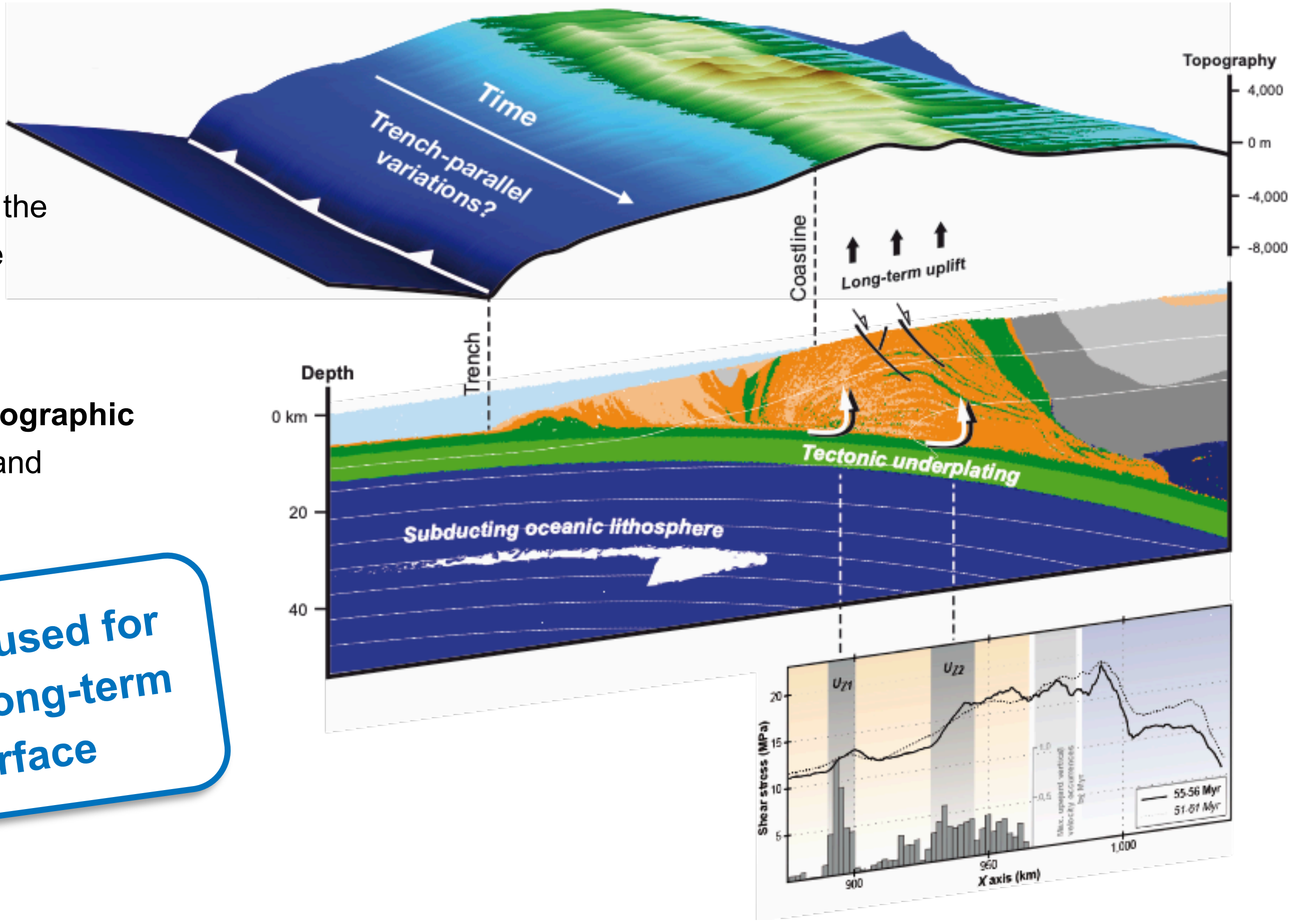

3D shape of fore-arc topography can be used for tracking deep accretion processes and long-term frictional properties of the plate interface

More details on this study

Menant A., Angiboust S., Gerya T. (2019), Stress-driven fluid flow controls long-term megathrust strength and deep accretionary dynamics, *Sci. Rep.* **9**(9714).

Menant A., Angiboust S., Gerya T., Lacassin R., Simoes M., Grandin R. (2020), Transient stripping of subducting slabs controls periodic forearc uplift, *Nat. Commun.* **11**(1823).

Supplementary Material

Field evidence of tectonic underplating: **coherent tectonic slices in a fluid-rich environment**

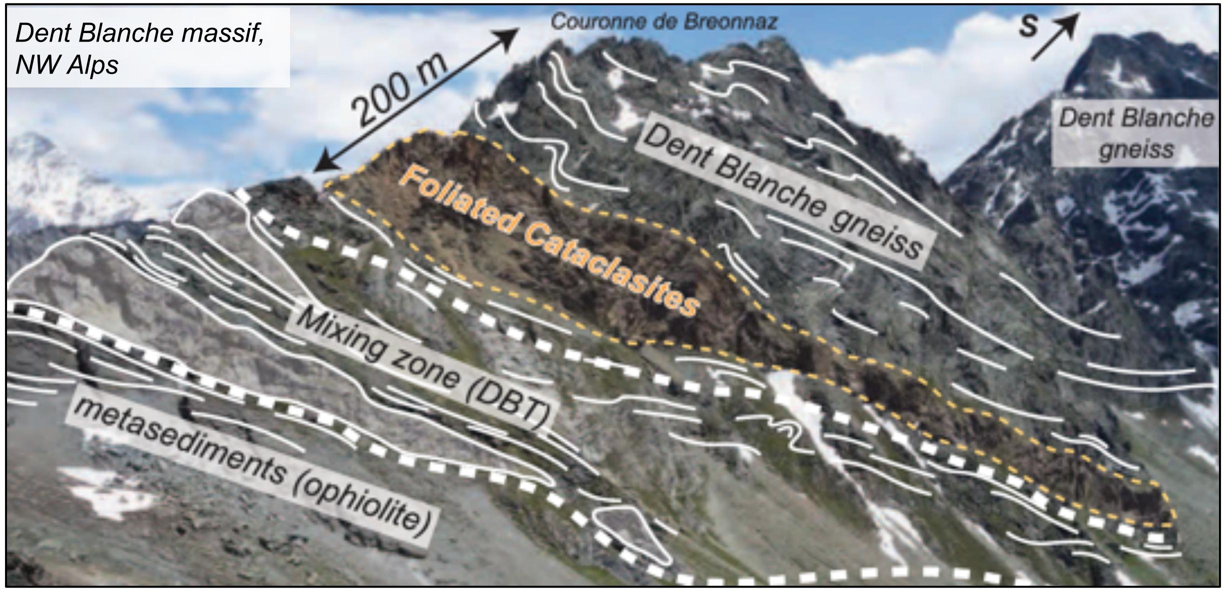

[*Angiboust et al.*, 2015]

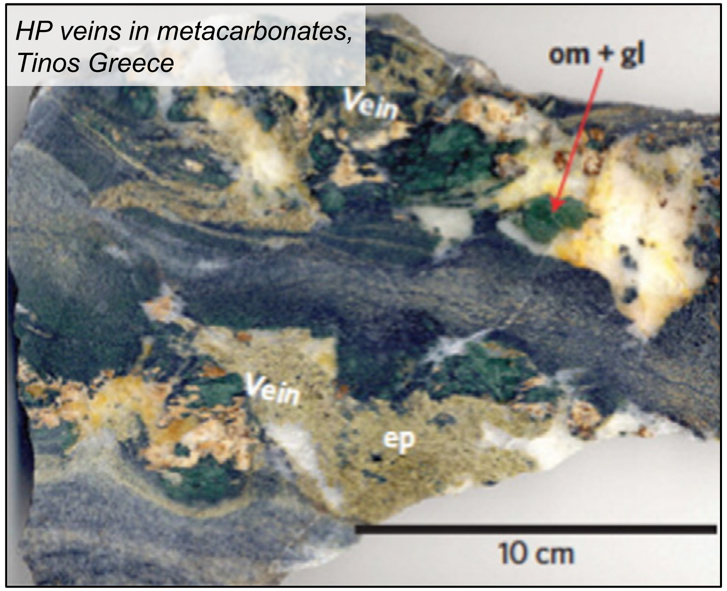

[*Ague & Nicolescu*, 2014]

Evidence from **geophysical observations**

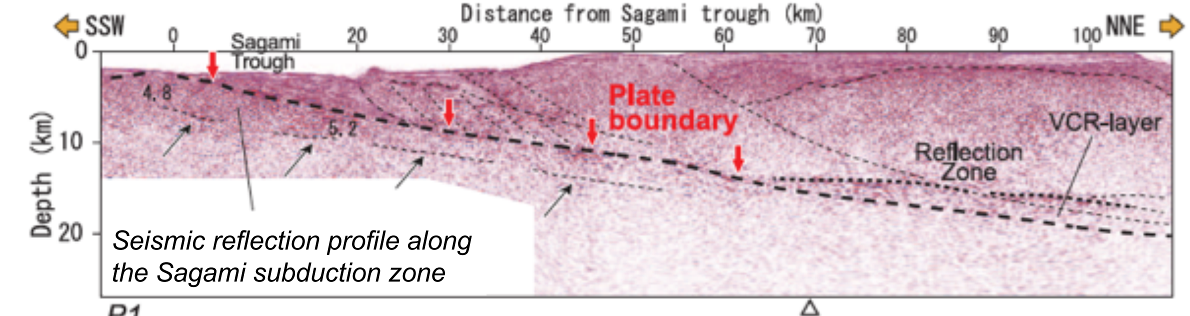

[*Kimura et al.*, 2010]

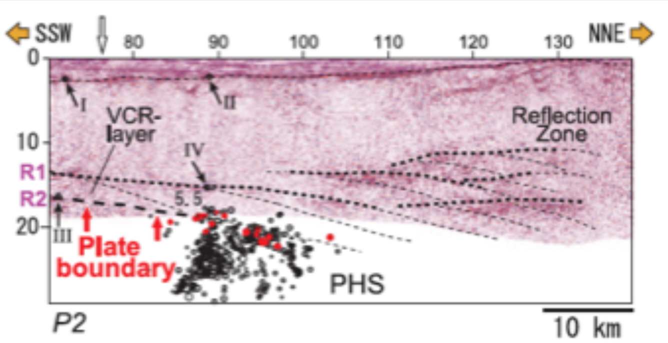

Modelling strategy

- **High-resolution thermo-mechanical models** of ocean-continent subduction by solving mass, momentum and heat conservation equations, using a marker-in-cell technique [*Gerya* & *Yuen*, 2007]
- **Visco-elasto-plastic rheologies** constrained by laboratory experiments
- **Fluid (de)hydration and transport** (as Lagrangian markers) + **fluid-induced rheological weakening**

Model resolution

Grid size
x = 500 m
y = 370 m

and 8,209,600 markers

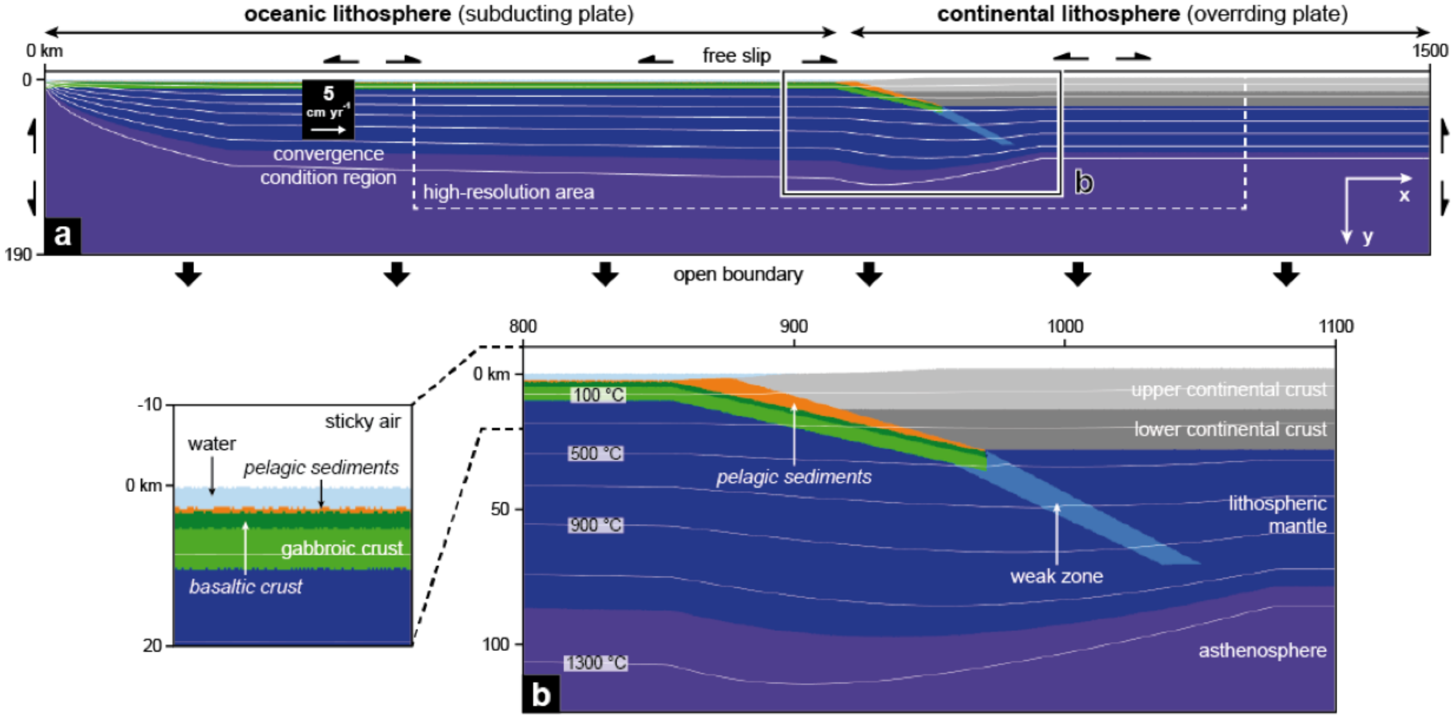

- **~80 experiments** by varying first-order parameters (e.g., convergence rate, thermal structure, amount of sediments, fluid-weakening effect)

Implementation of fluid processes

2. Transport

Reference percolation velocity

Pressure gradient

$$v_{i_{water}} = v_i + v_{perc}\, k_i, \qquad k_i = \frac{\rho_{crust}\, g_i - \dfrac{\partial P}{\partial x_i}}{(\rho_{crust} - \rho_{fluid})\, g_y},$$

Stokes flow

Fluid buoyancy

1. Dehydration

3. Hydration

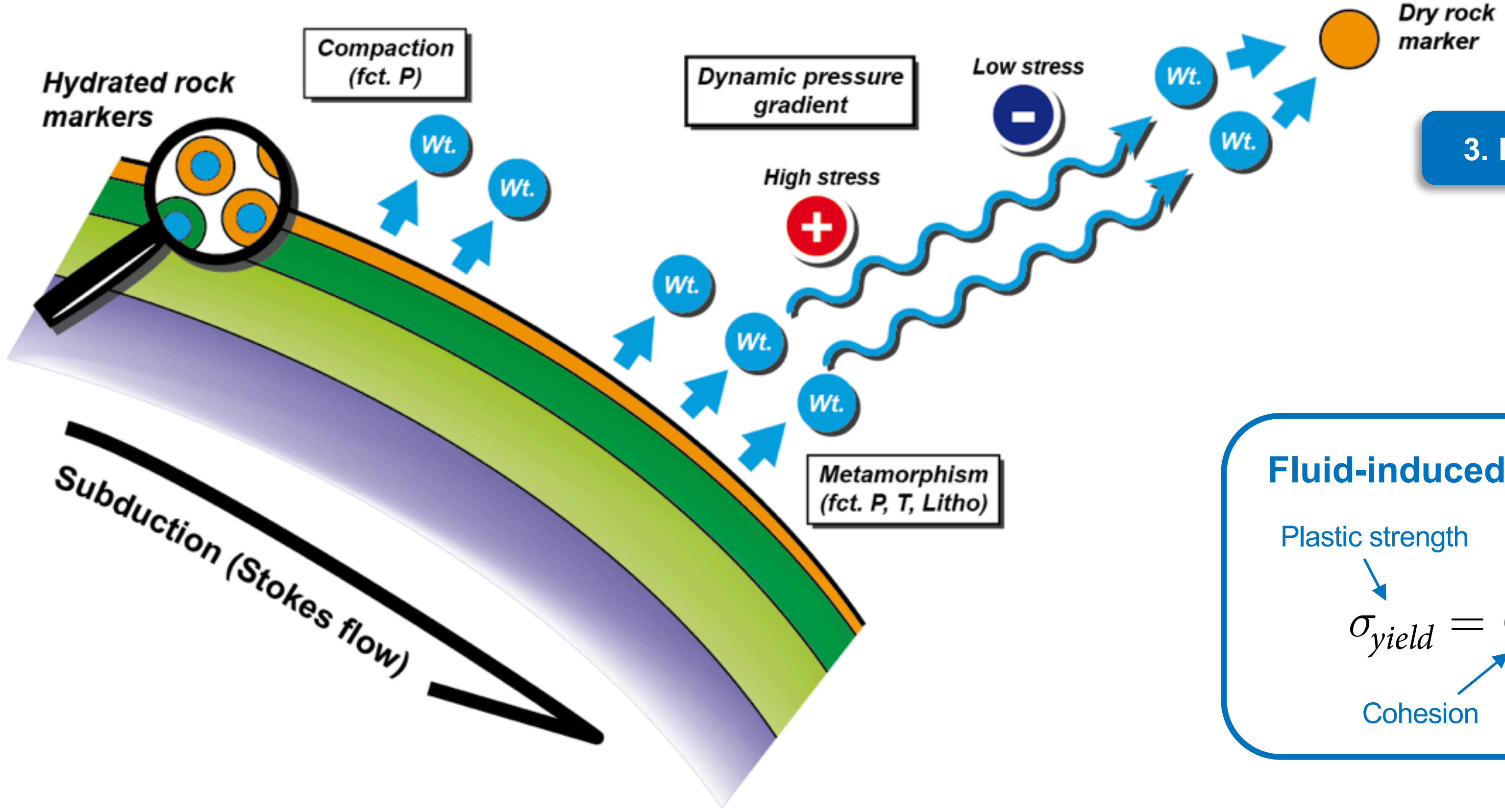

Fluid-induced rheological weakening

Plastic strength

Pore fluid pressure factor

$$\sigma_{yield} = C + P \sin(\varphi_{dry})\,(1 - \lambda_{fluid})$$

Cohesion

Friction coefficient

Accretive forearc margin in alternative models

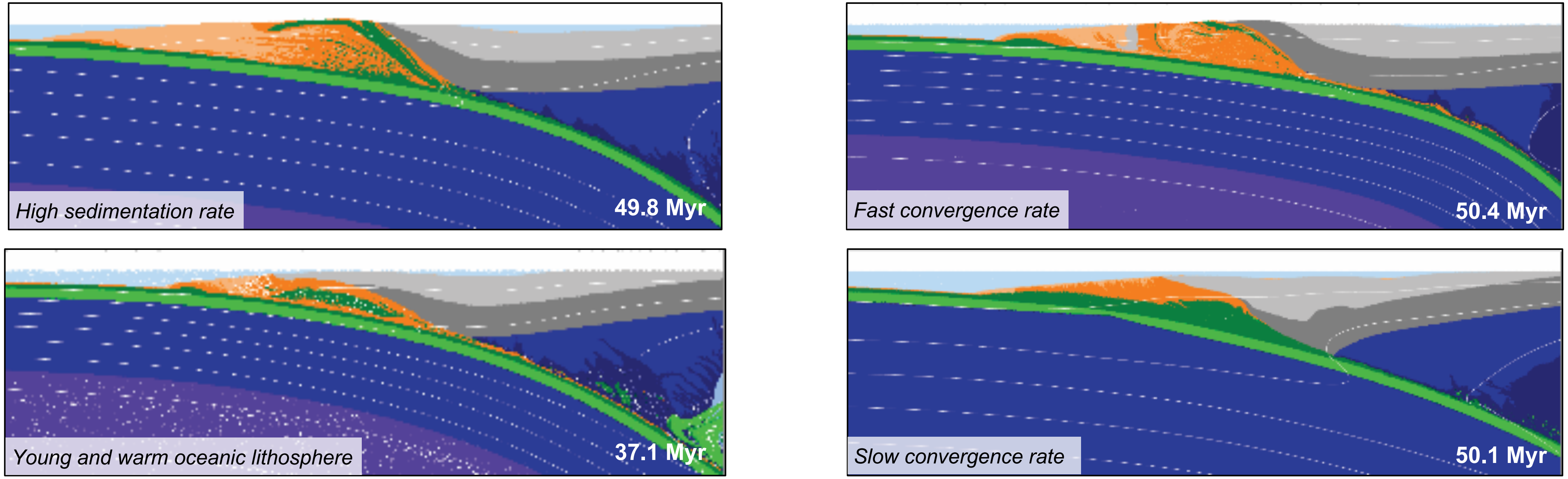

Sticky air
Water
Terrigenous sediments
Pelagic sediments
Basaltic crust
Gabbroic crust
Upper continental crust
Lower continental crust
Lithospheric mantle
Asthenosphere
Serpentinized mantle
Hydrated mantle

Erosive forearc margin

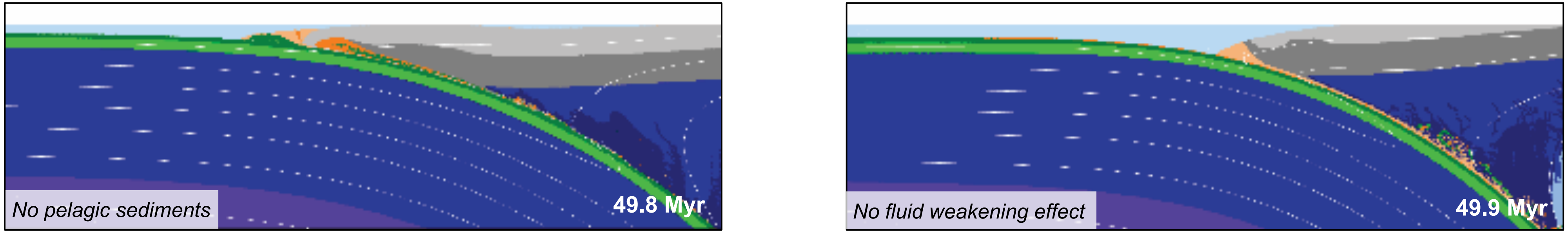

[*Menant et al.*, 2019; 2020]

Comparison of the reference experiment with the **H*P*-L*T* Western Series**, central-south Chile

- Predicted duplex geometry

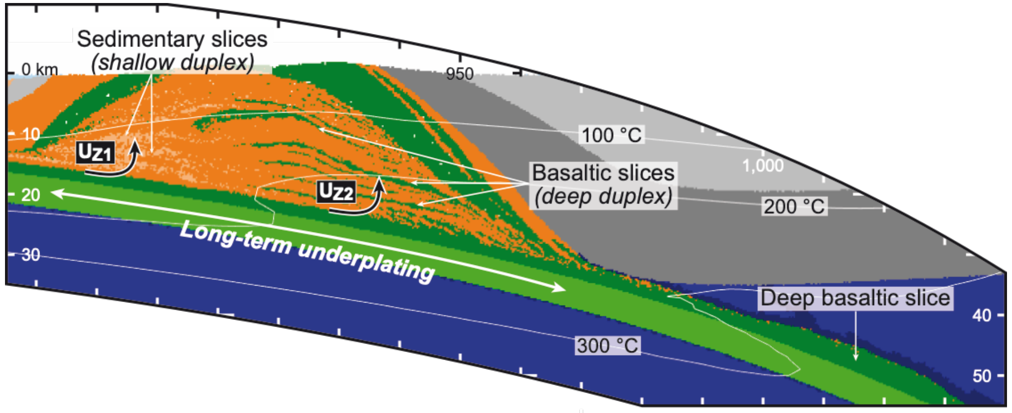

[*Menant et al.*, 2019]

- Geometry of the Chilean margin during the formation of the Western Series accretionary complex

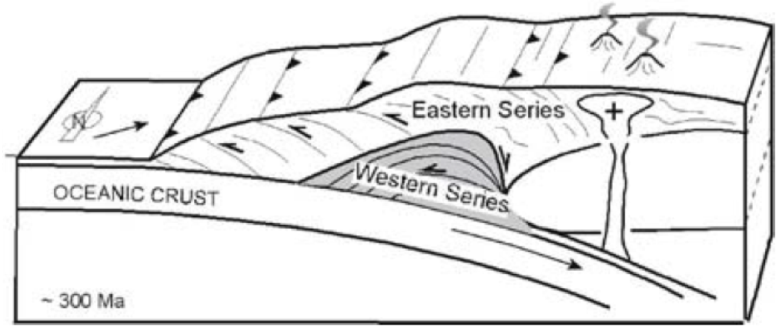

[*Glodny et al.*, 2006]

- Dome-like structure imaged below the Coastal Cordillera where the Western Series crops out

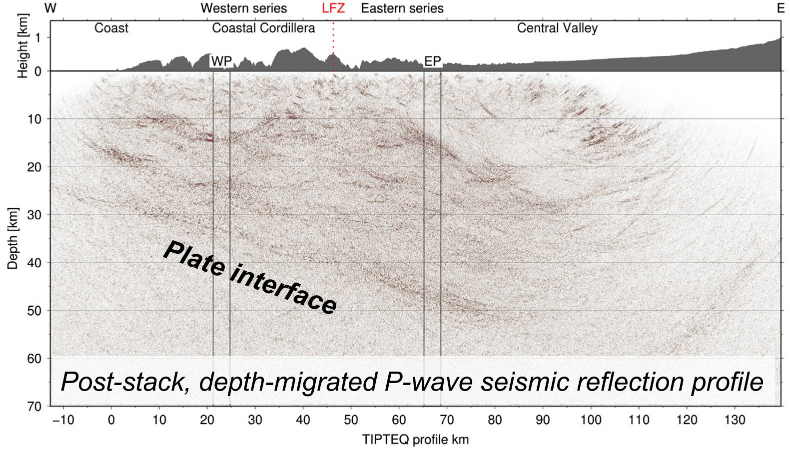

Post-stack, depth-migrated P-wave seismic reflection profile [*Ramos et al.*, 2018]

- Similar *P*-*T* peak conditions for H*P*-L*T* metamorphic rocks and exhumation rate (i.e., 0.2-0.6 mm/yr) [*Willner*, 2005]

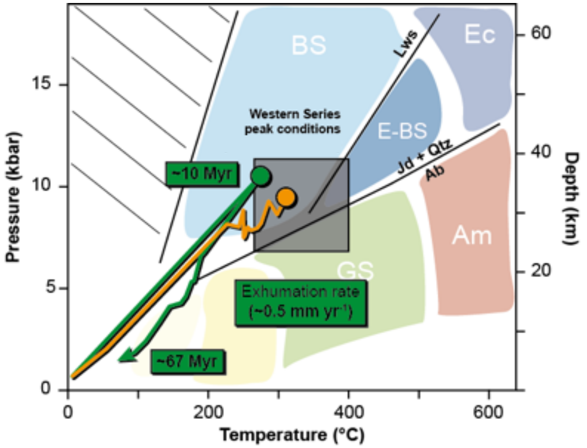

Predicted **forearc deformation** associated with tectonic underplating

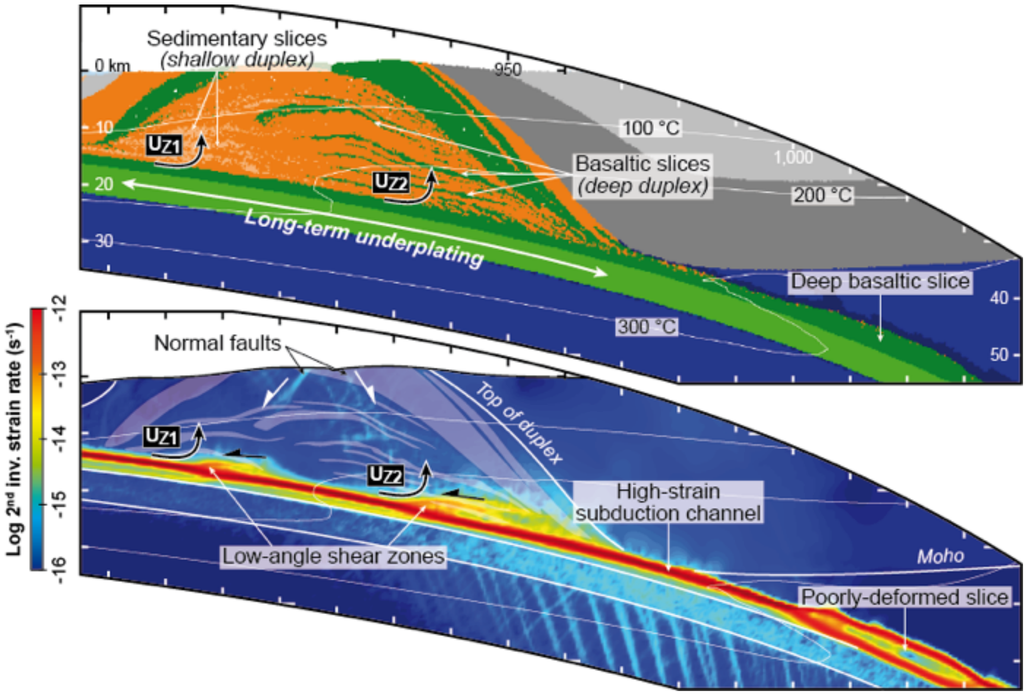

- **Compressional stress regime** at the base of the forearc domain
  = **insertion of tectonic slices** at the base of the duplex
- **Extensional stress regime** at shallow depth
  = **rock exhumation and doming of the forearc crust**

Pressure gradients and calculated fluid flow

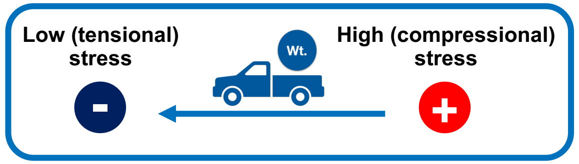

- Fluid trajectories and differential stress

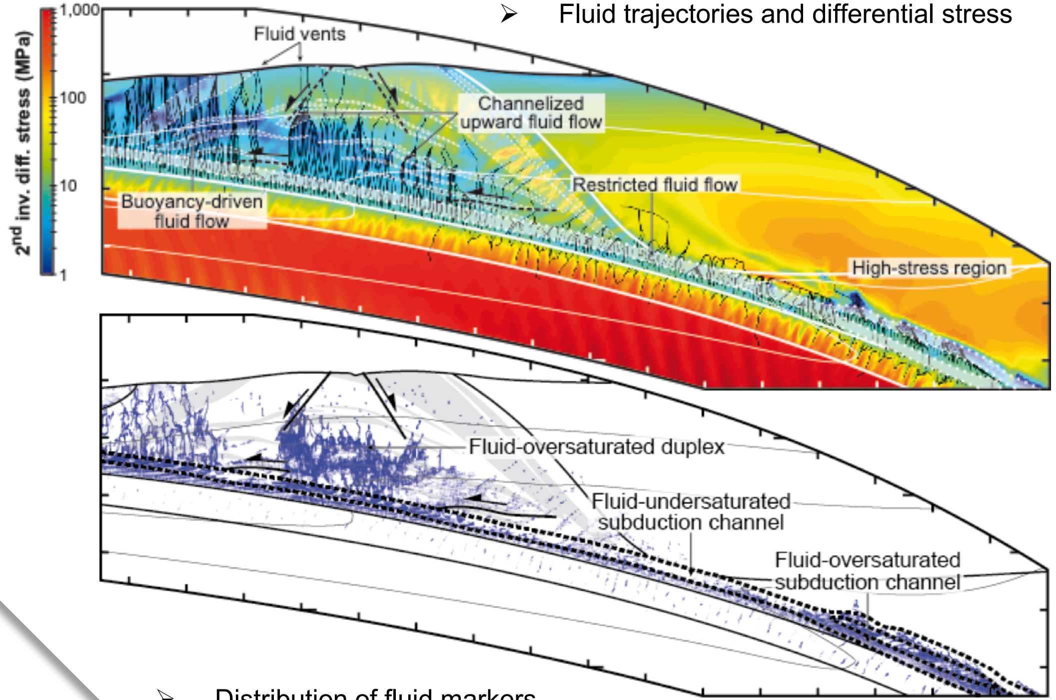

- Distribution of fluid markers

[*Menant et al.*, 2019]

Forearc geometry, topography and mass flow in alternative models

- Fast convergence rate (~8 cm/yr), **vertical overall mass flow**

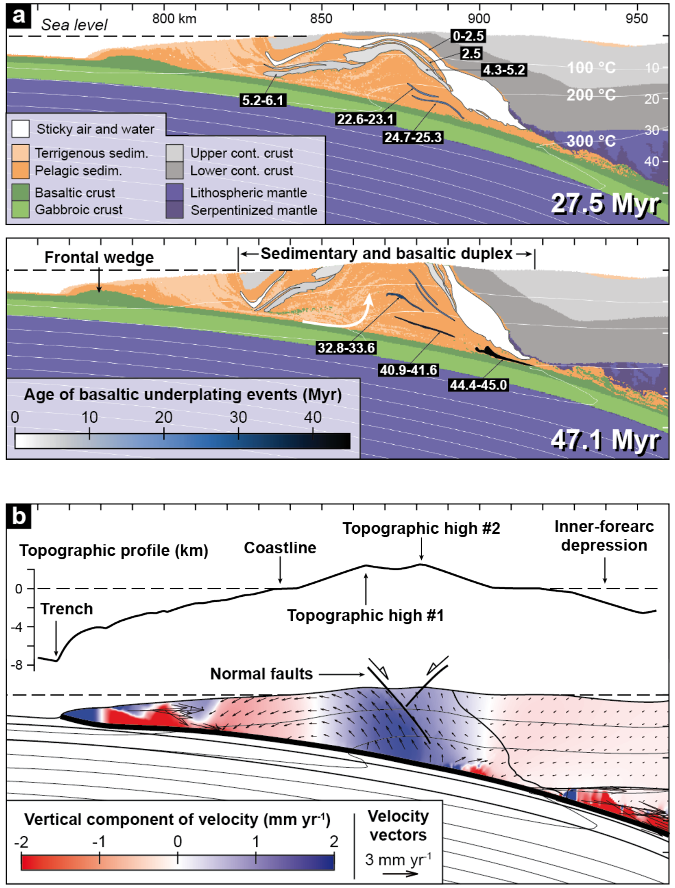

= **high coastal topography**

- Slow convergence rate (~2 cm/yr), **horizontal overall mass flow**

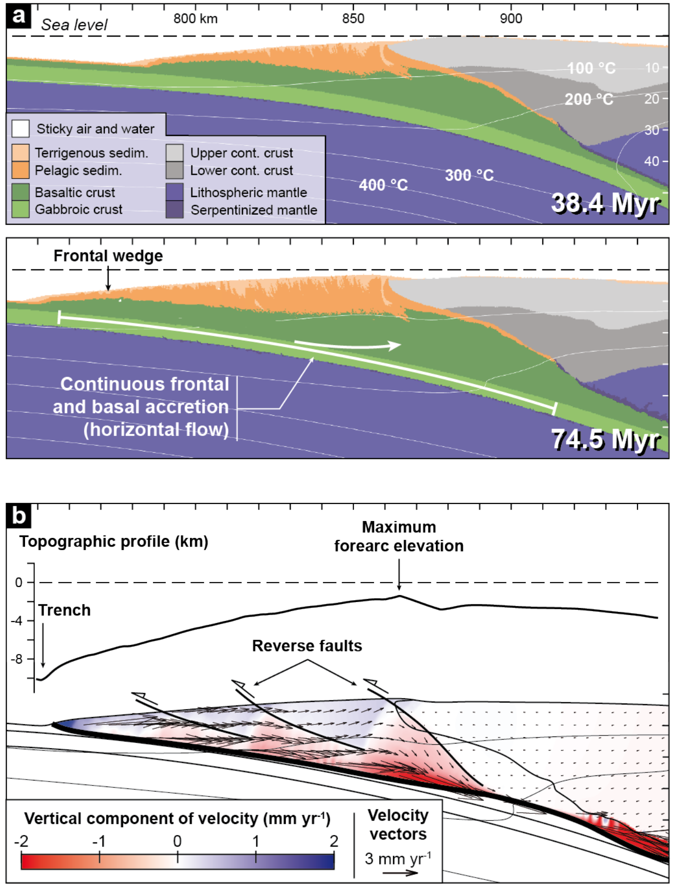

= **low coastal topography**

- No pelagic sediments, **minor forearc flow/deformation**

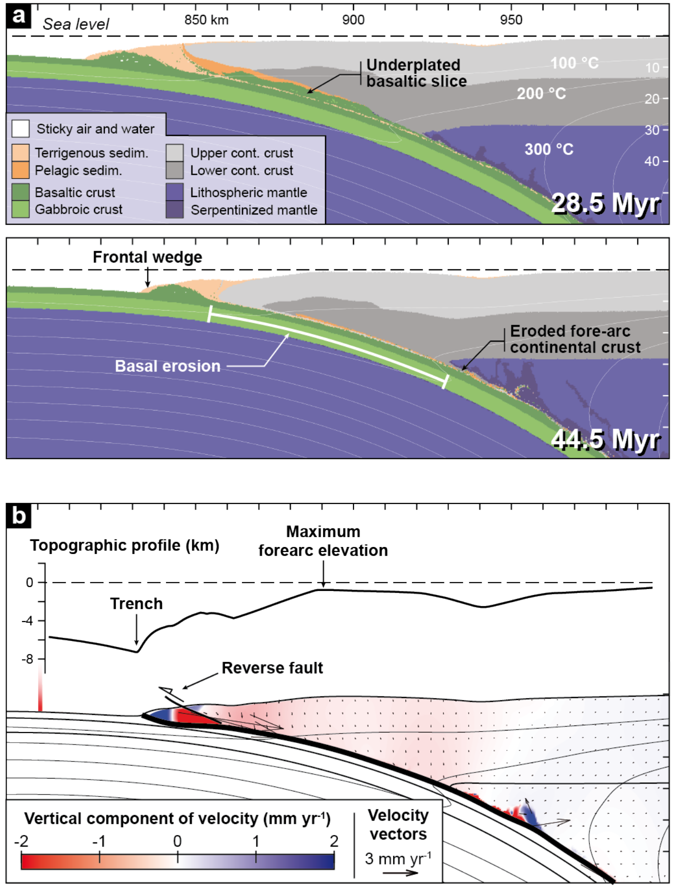

[*Menant et al.*, 2020]

= **low coastal topography**

Topographic signal in alternative models

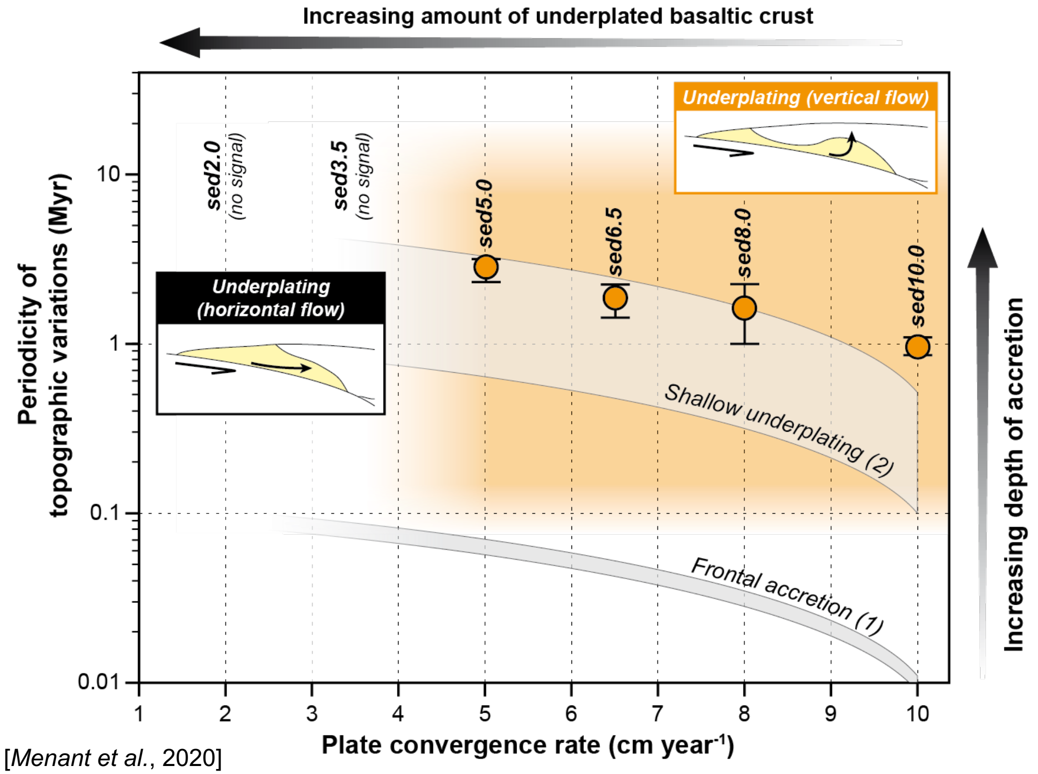

[*Menant et al.*, 2020]

- **Periodic vertical surface oscillations** are predicted when tectonic underplating is achieved through a **vertical mass flow**
- **Topographic signal reflects deep accretion dynamics**
- **The faster the plate convergence rate, the shorter the periodicity of topographic signal**
(i.e., fast kinematics allows faster stress build-up along the plate interface and rapid underplating)
- **The deeper the accretion event, the longer the periodicity of topographic signal**. See sandbox experiments of frontal accretion [*Hoth et al.*, 2007] and shallow underplating [*Lohrmann et al.*, 2006]
(i.e., reflecting the increase of rock failure threshold with depth)

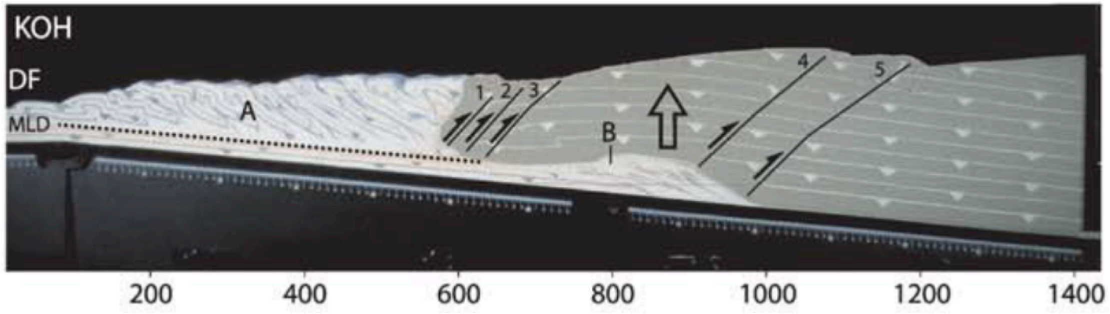

[*Lohrmann et al.*, 2006]

Trench-parallel variations in forearc topography as a proxy for temporal variations?

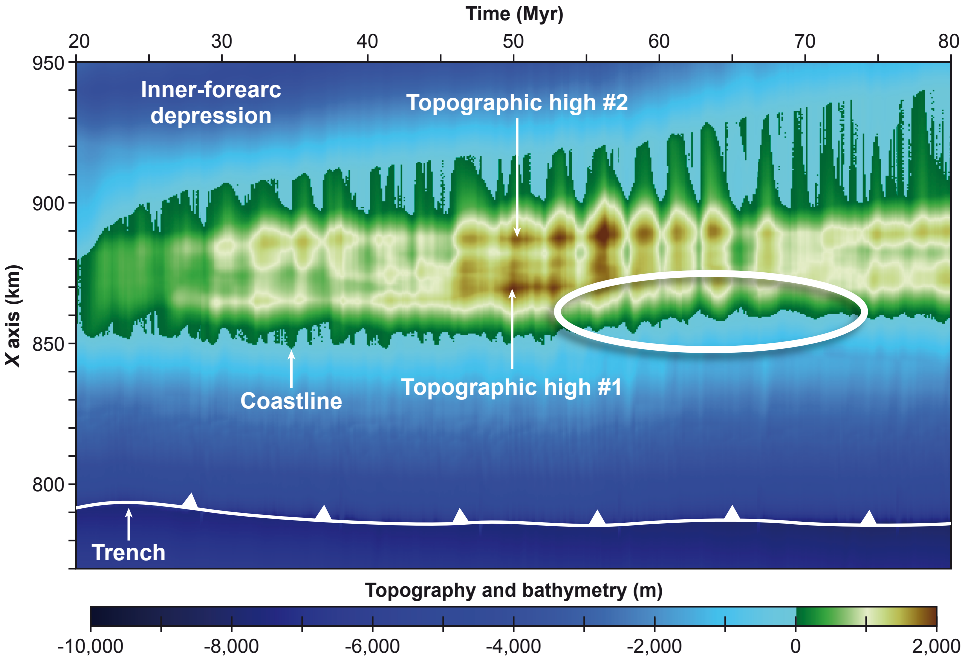

- Temporal variations of forearc topography predicted in the model: **uplift events associated with trenchward migration of the coastline**

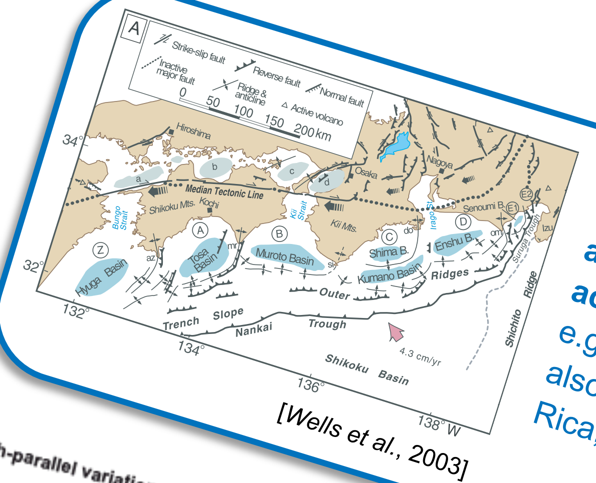

[Wells et al., 2003]

Peninsula/basin alternation along active margins, e.g., SW-Japan (but also Chile, Costa Rica, …)

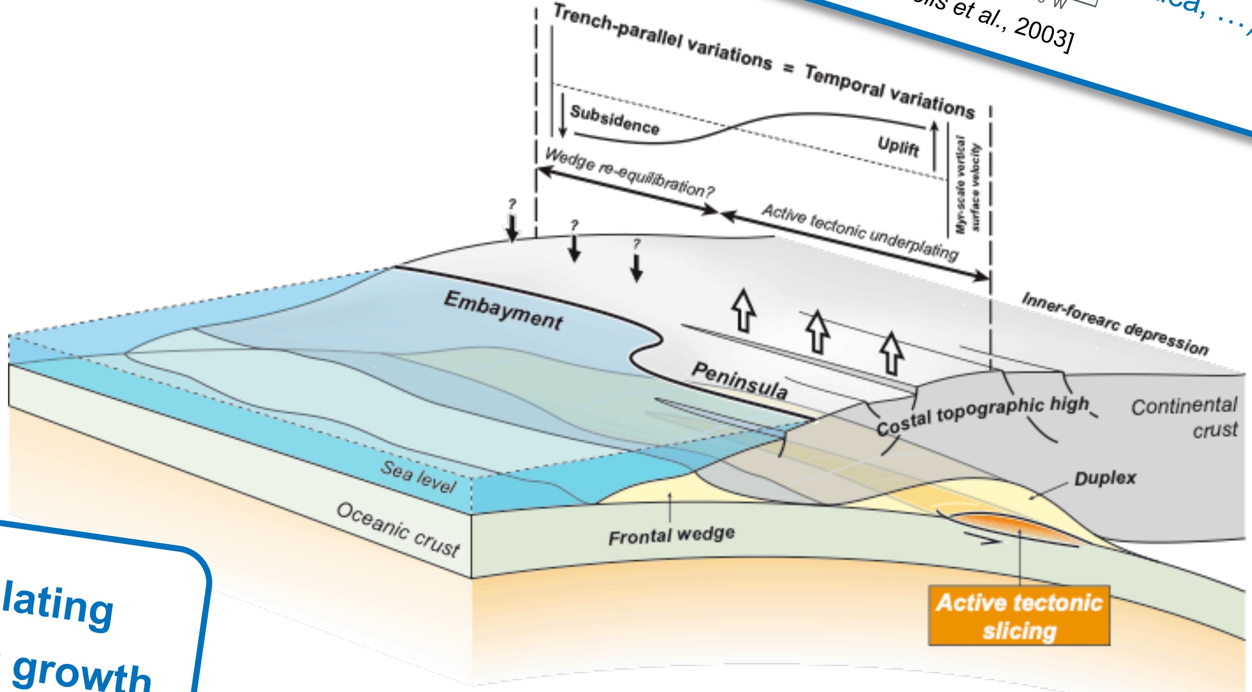

[Menant et al., 2020]

Underplated tectonic slices with a limited lateral extend

Peninsula ⟷ active tectonic underplating

Coastal Cordillera ⟷ long-term duplex growth

More details on this study

Menant A., Angiboust S., Gerya T. (2019), Stress-driven fluid flow controls long-term megathrust strength and deep accretionary dynamics, *Sci. Rep.* **9**(9714).

Menant A., Angiboust S., Gerya T., Lacassin R., Simoes M., Grandin R. (2020), Transient stripping of subducting slabs controls periodic forearc uplift, *Nat. Commun.* **11**(1823).

Additional references

Ague J. J., Nicoleascu S. (2014) Carbon dioxide released from subduction zones by fluid-mediated reactions, *Nat. Geosci.* **7**.

Angiboust S., Kirsch J., Oncken O., Glodny J., Monié P., Rybacki E. (2015), Probing the transition between seismically coupled and decoupled segments along an ancient subduction interface, *Geochem. Geophys. Geosyst.* **16**, 1905-1922.

Angiboust S., Cambeses A., Hyppolito T., Glodny J., Monié P., Calderón, Juliani C. (2018), A 100-m.y.-long window onto mass-flow processes in the Patagonian Mesozoic subduction zone (Diego de Almagro Island, Chile), *Geol. Soc. Am. Bull.* **130**(9-10).

Bassett D., Watts A. B. (2015), Gravity anomalies, crustal structure, and seismicity at subduction zones: 2. Interrelationships fore-arc structure seismogenic behavior. *Geochem. Geophys. Geosyst.* **16**, 1541–1576.

Encinas A., Finger K. L., Nielsen S. N., Lavenu A., Buatois L. A., Peterson D. E., Le Roux J. P. (2008) Rapid and major coastal subsidence during the late Miocene in south-central Chile, *J. South Am. Earth Sci.* **25**, 157-175.

Gerya T. V., Yuen D. A. (2007), Robust characteristics method for modelling multiphase visco-elasto-plastic thermo-mechanical problems, *Phys. Earth Planet. Inter*. **163**, 83–105.

Glodny J., Echtler H., Figueroa O., Franz G., Gräfe K., Kemnitz H., Kramer W., Krawczyk C., Lohrmann J., Lucassen F., Melnick D., Rosenau M., Seifert W. (2006), Long-Term Geological Evolution and Mass-Flow Balance of the South-Central Andes, in: *The Andes* (eds. Oncken O. et al.), Springer, Berlin, Heidelberg.

Hoth S., Hoffmann-Rothe A., Kukowski N. (2007), Frontal accretion: an internal clock for bivergent wedge deformation and surface uplift. *J. Geophys. Res.* **112.**

Kimura H., Takeda T., Obara K., Kasahara K. (2010), Seismic evidence for active underplating below the megathrust earthquake zone in Japan, *Science* **329**, 210–212.

Lohrmann J., Kukiwski N., Krawczyk C. M., Oncne O., Sick C., Sobiesiak M., Rietbrock A. (2006), Subduction Channel Evolution in Brittle Fore-Arc Wedges – a Combined Study with Scaled Sandbox Experiments, Seismological and Reflection Seismic Data and Geological Field Evidence, in: *The Andes* (eds. Oncken O. et al.), Springer, Berlin, Heidelberg.

Ramos C., Mechie J., Stiller M. (2018), Reflection seismic images and amplitude ratio modelling of the Chilean subduction zone at 38.25°S, *Tectonophysics* **747**(748), 115-127.

Wells R. E., Blakely R. J., Sugiyama Y., Scholl D. W., Dinterman P. A. (2003), Basin-centered asperities in great subduction zone earthquakes: a link between slip, subsidence, and subduction erosion? *J. Geophys. Res. Solid Earth* **108**.

Willner A. P. (2005) Pressure–temperature evolution of a late Palaeozoic paired metamorphic belt in North–Central Chile (34°–35°30′S), *J. Pet.* **46**, 1805–1833.